Analysis of Holographic Interferograms of Aerodynamic Models in a Wind Tunnel

(NASA-CR-177006) ANALYSIS OF HOLOGRAPHIC INTERFEROGRAMS OF AERODYNAMIC MODELS IN A WIND TUNNEL Final Report, 1 May 1984 - 31 Dec. 1985 (University of the Pacific) 41 p CSCL 14E G3/35

N86-29197

Unclas 43302

University of the Pacific
3601 Pacific Avenue
Stockton, California 95211

Richard L. Perry
Principal Investigator
Physics Department

Final Report
Covering the Period
May 1, 1984 to December 31, 1985
Cooperative Agreement No. NCC 2-298

George Lee
NASA Technical Officer
NASA-Ames Research Center
Moffett Field, CA 94035

Analysis of Holographic Interferograms of Aerodynamic Models in a Wind Tunnel

University of the Pacific
3601 Pacific Avenue
Stockton, California 95211

Richard L. Perry
Principal Investigator
Physics Department

Final Report
Covering the Period
May 1, 1984 to December 31, 1985
Cooperative Agreement No. NCC 2-298

George Lee
NASA Technical Officer
NASA-Ames Research Center
Moffett Field, CA 94035

TABLE OF CONTENTS

ANALYSIS OF HOLOGRAPHIC INTERFEROGRAMS OF AERODYNAMIC MODELS IN A WIND TUNNEL

Introduction

Wind tunnels are used extensively in aerodynamic research to study the air flow over the surfaces of models. (It is preferable to test and improve the aerodynamic characteristics of models of new aircraft designs in a wind tunnel before committing a test pilot to a full scale experimental aircraft for reasons of both safety and economy.) The data include the pressures, velocities, and densities of the air in the vicinity of the model. Unfortunately most of the techniques for measuring these properties introduce perturbations into the air flow and thus influence the measurements. Also they are tedious or time-consuming. If the measurements take much time, subtle changes in the operating conditions of the wind tunnel may occur during the test which could degrade the reliability of the data. The ideal method for obtaining the required data would be instantaneous and it would not disturb the air flow.

Holographic Interferometry is a new non-invasive technique for estimating variations in the air density distribution in a test region. The application of this technique to aerodynamics has been under development for almost two decades[1,2]. The only probe is laser light and this does not perturb the air flow. The holograms are taken quickly (15-20 nanoseconds) through the use of pulsed lasers. This is important not only for the above reason, but also for many applications such as studying unsteady flow phenomena where this technique is the only one capable of recording the data. The technique of holographic interferometry records the entire flow field by "freezing" the information in an instant of time

like taking a picture. The testing of this method with a two-dimensional wing (figure 1) has been reported.[3]

This experiment is a long-term project to test the ability of holographic interferometry to provide fringe data of sufficient accuracy that the air density distribution around a three-dimensional aerodynamic model in a wind tunnel can be determined accurately. The experiment using a three dimensional model is much more difficult to analyze than that using a two dimensional model since data in three dimensions are recorded on a two dimensional plate. The holograms and interferograms were made prior to this report period. The fringe distributions for several cases were determined during this report period and the data analysis and calculations have begun. This report will describe work from previous report periods so that the description of the latest work can be more readily understood. A good introduction to this technique is given in chapters 5 and 6 of the book by Vest.[2]

Experimental Procedure

The "holocamera" that was constructed for the 2 foot by 2 foot transonic wind tunnel at Ames Research Center[4] is diagramed in Figure 2. It was designed to use the two schlieren mirrors that were already mounted with one on either side of the wind tunnel test section. The light source was a Nd:YAG pulsed laser using a frequency doubler so that its output was 532 nm in the green part of the spectrum. The laser was enclosed in a metal box designed to prevent the escape of any stray light. The beam was directed upward through a small opening into a second metal box where it was passed through first a spatial filter and then a beamsplitter. The beamsplitter divided the laser beam into two components--the "object beam"

and the "reference beam". The object beam was reflected from the front surface of the beamsplitter through a system of lenses and mirrors to the first schlieren mirror from which it was then reflected as a collimated or parallel beam about 1½ feet in diameter through the test chamber where the aerodynamic model was located and on to the second schlieren mirror. The object beam was then reflected from the second schlieren mirror to another system of lenses and mirrors which formed it into a collimated beam about 2½ inches in diameter which was recorded on a holographic film plate. Meanwhile, the reference beam passed through the beamsplitter to a series of mirrors which reflected it down a tube, through a trench under the wind tunnel, and up a tube to a lens system which formed it into a collimated beam about 4 inches in diameter which was centered over the object beam at the holographic film plate. Thus the film plate was exposed by both beams simultaneously. Note that care was taken to collimate the object beam as it passed through the wind tunnel and to collimate both beams in the region where they were brought together at the film plate. The holograms were recorded on Agfa-Gaevert 10E75 HOLOTEST 4" x 5" glass film plates. Care was also taken to ensure that the total optical path lengths of both beams were the same to within a few inches.

The laser could be operated at low power output at about 10 pulses per second for beam alignment purposes. After the beams were properly aligned the laser was triggered one pulse at a time at high power output to make the holograms. Each pulse was about 20 nanoseconds long. The laser could also be "double pulsed" at high power output with a time interval of about 50 nanoseconds between the pulses but this mode was seldom used.

The spatial filter in front of the beamsplitter had two functions. First, the usual function of a spatial filter was to remove unwanted

"optical noise" from the laser beam such as diffraction patterns caused by specks of dust and imperfections in the various optical elements ahead of the spatial filter. A more important function of the spatial filter in this experiment was the reshaping of the laser beam since the beam as it leaves this laser has a cross-sectional shape somewhat similar to a doughnut. There was very little light in the center of the beam, but there was a ring of intense light around the center. As the beam progressed some distance from the laser the light intensity was gradually redistributed so that the central dark region was filled in. Holography works best when the beam has a "Gaussian" cross-section, i.e., the central portion of the beam must be the most intense with the intensity decreasing smoothly toward the edge of the beam. The spatial filter is basically a very small pinhole in a sheet of stainless steel. The pinhole was placed far enough along the beam so that it enhanced the redistribution of the central portion of the beam intensity. The optimum position of the pinhole was obtained when circular fringes were observed symmetrically around the bright central portion of the beam.

Each run at the wind tunnel was begun by mounting the aerodynamic model in the desired orientation in the test chamber and closing the wind tunnel. The laser was turned on and warmed up. The laser beam was lined up through the various optical elements so that an optimum signal reached the hologram plate by both beams. This was often a tedious procedure because of the sensitivity of the interaction between the beam and the optical elements (especially the pinhole), the long distances that the beam had to travel and the tendency of the beam position to drift slightly as it left the laser. When the proper alignment was obtained several holograms were made at the "no air flow" condition before the wind tunnel was started.

These holograms were called "reference" holograms because there was no disturbance in the air around the model so that the laser beam passed through the test chamber unchanged. The wind tunnel was then turned on so that the air speed was usually at a mach number of $M_\infty = 0.6$ or $M_\infty = 0.8$ for the cylindrical model with a hemispherical nose or $M_\infty = 1.25$ or $M_\infty = 1.30$ for the pointed model with the symmetrical bump. When the desired operating condition was reached several holograms were made. These were called "object" holograms because they recorded the desired data, i.e., the disturbances in the air around the model. Holograms were exposed for each of the desired wind speeds at this orientation. The wind tunnel was then turned off and after the air stopped moving several more reference holograms were made. The wind tunnel was then opened, the orientation of the model was changed, the tunnel was closed and the next run was made. For three dimensional models it was necessary to make a series of holograms around the model just like in a "CAT" scan. Due to the symmetry of these models, only ten views made at ten degrees apart were needed. The model was rotated rather than changing the direction of the laser beam. When everything was functioning properly the wind tunnel could reach the desired operating conditions in from five to fifteen minutes depending on which condition was desired and since each set of holograms could be made in a minute or two a data run could be made in a fairly short time. The exposed film plates were taken to a dark room, removed from their holders, developed and dried.

Many holograms were made during the course of this project using several models. These models included primarily a 5.08 cm (2 inch) diameter cylinder with a hemispherical cap usually run at mach numbers of 0.60 and

0.80 for both axisymmetric and 5½ degree angle of attack cases and a 5.08 cm (2 inch) diameter symmetrical sharp nosed model with a small "bump" around its midsection run at mach numbers of 1.25 and 1.30. The cylinder with cap model was also run in the axisymmetric mode at mach numbers of 0.70 and 0.85. Also tested at mach numbers of 1.25 and 1.30 was a sharp pointed model with a small bump on one side similar to a canopy. Finally, a test was made at mach numbers of 0.60, 0.70, 0.80 and 0.85 in the axisymmetric mode using a 5.08 cm (2 inch) diameter cylinder with a hemispherical cap made of clear plastic instead of the stainless steel that was used for the other models.

The holograms must be reconstructed so that the data may be obtained from them. This was done in a laboratory after the runs were completed. Figure 3 shows a diagram of the reconstruction apparatus as it was set up on an optical table. The light source was a one watt argon ion laser emitting a continuous green light at 514.5 nanometers which is nearly the same wavelength as that emitted by the Nd:YAG pulsed laser so the distortion caused by the difference in wavelength is negligible. This laser beam was directed by mirrors to a lens system which expanded and collimated it before it reached the hologram plates. Two holograms for each test condition were mounted in tandem in a special dual plate holder with the object plate approximately 0.508 cm behind the corresponding reference plate. (The object plate holder had been mounted behind a 0.508 cm spacer during the exposure at the wind tunnel.) Most of the reconstruction beam intensity passed straight through the plates and was blocked. A small portion of the reconstruction beam intensity was diffracted to one side and this carried the desired reconstructed image from each hologram through a focus-

sing lens, diaphragm and shutter to a camera back with a ground glass screen where the image could be observed and photographed. One of the plates was moved with respect to the other using micrometer screws on the dual plate holder until the two shadows of the model reconstructed from the two plates matched. A magnifier was used to check this match and then to look for interference fringes in the region around the model. Usually very fine fringes were found and the micrometer screws were adjusted to obtain "infinite" fringes which were large, widely spaced, and symmetrical about the sting axis, or the axis of the model for cases of zero angle of attack. The term "infinite fringe" implies that the fringe is infinitely wide, i.e., that the field of view is of uniform irradience, when there is no disturbance in the beam path. "Finite fringes" are usually parallel straight fringes that result when the object hologram is tilted slightly with respect to the reference holograms[2], when there is no disturbance in the beam path. If there is a disturbance in the beam path then the fringes are distorted. Photographs of infinite fringe interferograms are shown in Figures 4, 5 and 6a. A finite fringe interferogram is shown in Figure 6b.

The interferograms were digitized, i.e., the fringes were numbered and the fringe distribution given in terms of the y and z coordinates as shown in Figure 7. Initially this was done by hand for several axisymmetric cases. Then a semiautomatic technique for digitizing the interferograms was developed by Becker[5] which utilized a closed circuit television camera, a monitor, an image enhancement processor, and a computer. Several complete sets of interferograms of the models at 5½ degrees angle of attack were digitized on this system.

Since the computer analysis is made around the z-axis which is parallel to the air flow and since the origin of the coordinate system is at the

leading edge of the model, the z-axis and the origin must be carefully determined for each interferogram when the model is set at 5½ degrees angle of attack. The model will appear to be at anywhere from 0 degrees to 5½ degrees angle of attack in the interferogram depending on its orientation about the axis of the "sting mount" in the wind tunnel while at 5½ degrees angle of attack. The sting axis was oriented along the direction of the air flow. There were ten orientation angles at ten degree intervals from 0 degrees to 90 degrees about the sting axis.

Becker calculated the apparent angle of attack corresponding to each orientation angle. He made an overlay transparency consisting of an 80mm scale and a series of dots representing the apparent angles on a sheet of clear plastic. The transparency was placed over each interferogram so that the midpoint of the 80mm scale and the dot representing the appropriate apparent angle both were located along the axis of the model as shown in Figure 8. The interferogram and transparency combination was then mounted in front of the television camera which then recorded them in the computer and the image was displayed on the monitor. A cursor was moved over the image to locate the two endpoints of the 80mm scale and the leading edge of the model so that the computer could determine the location of coordinates and the directions of the y-axis and z-axis. Then the process of counting the fringes could begin. Note that no lines other than the scale could be drawn on either the interferogram or transparency since they would interfere with the processing done by the computer which would interpret them as fringes.

Theory

A light beam may be described as a sinusoidal electromagnetic wave

that travels through vacuum at a speed of $c = 2.998 \times 10^8$ meters per second. It is often more convenient, however, to describe a light beam as a ray of light especially as it passes through various optical elements such as windows and lenses. If the light beam travels through a transparent medium, its speed v will be less than c. The ratio of the two speeds is defined as the index of refraction of the medium, n:

$n = \frac{c}{v}$, and n is greater than 1.00 since v is less than c.

The distance, s, that the light ray actually travels in a certain time, t (in seconds), is given by

$s_o = ct$ in a vacuum, and by

$s = vt$ in a transparent medium.

There is another distance, however, that is of primary interest in interferometry. This is the optical path length of a light ray through a transparent medium and is defined as

$$\phi = \int n ds.$$

If we substitute for $n = c/v$ and $ds = vdt$ we find that

$$\phi = \int \left(\frac{c}{v}\right) (vdt) = \int cdt = c\int dt = ct = s_o.$$

Thus we see that the optical path length of a light ray through a transparent medium is exactly equal to the distance it would have traveled in a vacuum in the same length of time. This is important because of another fundamental relationship in wave motion which relates the speed, v, of the wave, its frequency, f, and its wavelength, λ:

$c = f\lambda_o$ in a vacuum, and

$v = f\lambda$ in a transparent medium.

If we multiply each speed by the same time we find

$$s_o = ct = f\lambda_o t = ft\lambda_o = N\lambda_o$$

$$s = vt = f\lambda t = ft\lambda = N\lambda$$

where N is the number of vibrations since the frequency $f = N/t$ is the number of vibrations per second and is independent of the medium that the wave is traveling through. Thus we see that in the same length of time the wave would have traveled the same number of wavelengths whether in vacuum or in any transparent medium. Another relationship can be obtained from the last two sets of equations:

$$ct = N\lambda_o \quad \text{and} \quad vt = N\lambda,$$

$$\frac{t}{N} = \frac{\lambda_o}{c} \quad \text{and} \quad \frac{t}{N} = \frac{\lambda}{v}.$$

Then $$\frac{\lambda_o}{c} = \frac{\lambda}{v} \quad \text{or} \quad \frac{\lambda_o}{\lambda} = \frac{c}{v} = n$$

so $$\lambda = \frac{1}{n}\lambda_o.$$

This shows that the wavelength of the light wave of a certain frequency in a transparent medium is shorter than its wavelength would be in a vacuum since n is greater than 1.00.

In both interferometry and holography the basic concept involves the combination of waves of the same frequency that originally were all in the same phase but which have traveled over different paths before they are brought together in a region where they interact with each other. According to the principle of superposition, at any point in the interaction region the net disturbance will be a vibration which at any instant will be the algebraic summation of the individual vibrations due to the individual waves passing that point (assuming that they all have the same polarization). If a recording device such as a photographic film is placed in the interaction region, it will record the net disturbance at its location. This can be illustrated by the Mach-Zehnder interferometer which is diagrammed in Figure 9.

A narrow beam of light from a small bright source, a laser in this example, is expanded by lenses into a uniform wide parallel beam. It is divided by a beamsplitter (division of amplitude) into two beams of equal optical path length which are brought back together where they interact. The resulting interference pattern can be observed visually on a screen or recorded on film. If the optical path lengths, Φ_1 and Φ_2 , of the two beams are exactly the same number of wavelengths, they will add together resulting in an interference maximum and the screen will appear bright. If one beam path is exactly one half wavelength longer than the other, the two waves will be out of phase so that they will cancel each other and the screen will appear dark. Usually, however, the beam paths are not ideally uniform, so a series of light and dark bands (called interference fringes) will be observed. The light fringes correspond to those regions where the optical path length difference $\Delta\Phi = \Phi_2 - \Phi_1$ between the two beams is a whole number of wavelengths resulting in an interference maximum while the dark fringes correspond to those regions where $\Delta\Phi$ is a whole number plus one half wavelengths resulting in a cancellation of the light. These fringes may be parallel straight lines or arcs of circles, but often they are very irregular, especially if the index of refraction in the test section is not uniform. The change from a bright fringe to an adjacent dark fringe corresponds to a change in the difference in optical path lengths of one half wavelength of light. This is a very small distance since λ_o is about 5×10^{-7} meter for green light. These concepts of interferometry are discussed in detail in most standard optics textbooks such as Jenkins and White[6], Hecht and Zajac[7], or Meyer-Arendt[8].

Holography is basically a sophisticated application of the Mach-Zehnder interferometer (compare the diagram of the holocamera of Figure 2 with the diagram of the Mach-Zehnder interferometer of Figure 9). Close examination

of a properly exposed and developed holographic film plate reveals that the gray color is actually very many fine light and dark interference fringes. When this hologram is placed in the reconstruction beam of Figure 3 so that the beam strikes the hologram at the same angle as the reference beam of the holocamera of Figure 2 the hologram will diffract a fraction of the beam to one side in somewhat the same way as a diffraction grating (See references 6, 7, or 8 for the theory of diffraction gratings.) at the same angle that the original object beam had been traveling. This diffracted (or reconstructed) beam carries essentially the same information as was in the object beam of the holocamera, such as the shadow of the aerodynamic model and the variations of the phase of the object beam waves due to the variations of the optical path length Φ through the test region around the model. This means that traditional wind tunnel techniques such as shadowgraphs and schlieren photographs can be made using the reconstructed beam from the hologram at any time in the laboratory.

Holographic Interferometry is a technique for finding differences between two holograms. In this experiment a pair of holograms for one orientation of the model were mounted in tandem in the dual plate holder with the reference (no flow) plate slightly in front of the corresponding object (air flow) plate as was discussed earlier. If the two plates are properly aligned so that the shadows of the model match exactly, the differences between the two holograms will reveal themselves as a pattern of light and dark fringes. These fringes indicate that the phases of the light waves that passed through the wind tunnel were changed by the air flow around the model.

The air flow around the model causes a variation in the air pressure and the air density around the model. The density of the air, ρ, is related to the index of refraction, n, of the air by the Gladstone-Dale equation:

$$n - 1 = K\rho \tag{1}$$

in which the Gladstone-Dale constant, K, is a property of the air that is almost independent of the temperature and pressure of the air and the wavelength of the light. This equation permits the determination of the density of the air if its index of refraction can be found. The index of refraction is related to the optical path length (defined earlier), Φ, of the light beam as it passes through the test section of the wind tunnel of width W by the equation

$$\Phi(y,z) = \int_{-\frac{W}{2}}^{+\frac{W}{2}} n(x,y,z)dx \tag{2}$$

where the coordinates are shown in Figure 7. Note that the origin of coordinates is at the leading tip of the model, the x-axis is the direction that the laser beam traveled through the test section of the wind tunnel, the y-axis is upward and the z-axis points in the direction of the air flow.

The index of refraction for no flow (the reference plate) is a constant, n_o, while the index of refraction with the air flow (the object plate) varies with the coordinates, n(x,y,z). When the two plates are reconstructed together in tandem to form an interferogram, the interference fringes are formed because of differences in the optical path length between the flow and no flow conditions:

$$\Delta\Phi(y,z) = \Phi(y,z) - \Phi_o(y,z) = \int_{-\frac{W}{2}}^{+\frac{W}{2}} [n(x,y,z) - n_o]dx. \tag{3}$$

For a bright fringe the optical path length difference is a whole number, N, of wavelengths, λ, while for a dark fringe it is a whole number plus one-

half wavelengths:

$$\text{Bright fringe:} \quad \Delta\Phi(y,z) = N\lambda \tag{4}$$

$$\text{Dark fringe:} \quad \Delta\Phi(y,z) = (N + \tfrac{1}{2})\lambda. \tag{5}$$

Combining equations and manipulating:

$$\Delta\Phi(y,z) = N\lambda = \int_{-\frac{W}{2}}^{+\frac{W}{2}} [n(x,y,z) - n_o]\,dx \tag{6}$$

$$N = \int_{-\frac{W}{2}}^{+\frac{W}{2}} \left[\frac{n(x,y,z) - n_o}{\lambda}\right] dx \tag{7}$$

$$N(y,z) = \int_{-\frac{W}{2}}^{+\frac{W}{2}} f(x,y,z)\,dx \tag{8}$$

where $N(y,z)$ is the distribution of the bright fringes obtained from the photographs of the interferograms and $f(x,y,z) = [n(x,y,z) - n_o]/\lambda$.

The unknown quantity that is desired, $n(x,y,z)$, is part of the function $f(x,y,z)$ that is inside the integral, while the known fringe distribution, $N(y,z)$, is outside the integral. Therefore equation (8) must be inverted. In the two-dimensional case, the properties in one direction (set up to be in the direction of the light beam) are constant and the integral is easily solved analytically. This is an important case since many aerodynamic flows, such as the flow about a wing, can be treated as two-dimensional. In the three-dimensional case, however, the inversion of the equation is much more difficult because the properties vary in all three directions. After investigating several inversion techniques, we chose to adapt the Fourier Transform method of Van Houten[9] to our experiment. His computer program has been extensively modified to meet our requirements. This method requires a number of views at equally spaced angles

around the field of interest. Van Houten's analysis using the inversion coordinates shown in figure 10 gives the following equation for $f(x_o,y_o)$ at a single point in one z-plane:

$$f(x_o,y_o) = \frac{1}{2\pi^2} \int_{-\frac{\pi}{2}}^{+\frac{\pi}{2}} \int_0^{\infty} [N(\rho_o+\rho,\theta) + N(\rho_o-\rho,\theta) - 2N(\rho_o,\theta)] \frac{d\rho}{\rho^2} d\theta. \qquad (9)$$

The appropriate values of N in this equation are taken from the fringe distribution obtained from the interferograms. The HOLOFT (Holographic Inversion by 2-D Fourier Transform) program will produce values of f(x,y) over the field of interest in each z-plane cross-section that is chosen, and it reduces these to the corresponding distributions of air density.

Results

The quality of the holograms varied greatly. Most of the holograms appeared to have a good exposure density with only a few being overexposed, but quite a few were underexposed or unevenly exposed. This underexposure was caused by a shift in the laser beam in the short time from when it was properly aligned to when the hologram was made. Apparently there was a slight instability in the laser itself which caused the beam to occasionally shift enough that it no longer passed through the pinhole in the optimum manner. Then usually the beam intensity was greatly reduced, but sometimes a portion of a diffraction ring was transmitted resulting in a non-uniform hologram.

Each of the holograms was tested individually by reconstructing it to determine its quality. A great variation of quality was found. Some reconstructions were very bright and many were good to fair in brightness, but there were also quite a few that were so faint that they were very difficult to see and for some no reconstructions were visible even though the exposure

looked fairly good. It is probable that vibrations at the wind tunnel degraded the fine interference fringes formed by the object and reference beams when the hologram was made.

The making of the interferograms during the reconstruction process is still largely an art. The pairs of holograms picked to form the interferograms were usually chosen on the basis of similar brightness, i.e., bright ones were paired together or faint ones were paired together so that the interference fringes would have good visibility. Pairing a bright one with a faint one would result in poor visibility in which the interference fringes would be very faint and difficult to see. In most cases it was possible to find pairs of holograms with reasonably similar brightness resulting in fringes of good visibility, but there were a few cases in which only faint fringes could be obtained. The proper alignment of the shadows of the model during the formation of an interferogram often proved to be difficult because one of the shadows would be considerably fainter than the other and thus difficult to see. This was especially true for the pointed models since the point was already difficult to see in most cases. Consequently it was found that many of the interferograms for the pointed models were not properly aligned. It may be necessary to repeat the reconstructions of the pairs which were the farthest from proper alignment in order to get a more reliable fringe distribution for these cases. Almost all of the interferograms for the cylinder with hemispherical cap were properly aligned with no mismatch of the shadows of the model.

The fringe structure in the interferogram is highly dependent on the settings of the micrometer screws of the dual plate holder. Just one turn of one of the screws can change the fringe structure from the broad infinite fringes to narrow finite fringes because the plates then become slightly misaligned. Even a slight adjustment can make a significant shift in the

location of the fringes without changing the basic shape of the fringes. The fringe at the tip of the model can be changed from bright to dark to bright while the other fringes move a considerable distance across the field of view, yet the fringe shape remains almost the same. This sensitivity of fringe location to a small change of adjustments does not appear to have much influence on the results since the distribution of the fringes remains about the same.

The analysis of the fringe structure in the case of the model of the two dimensional wing is quite straightforward since each fringe in the infinite fringe mode represents a contour of constant air density. In this two dimensional case equation (8) can be integrated easily since f is not a function of x. Thus a simple relationship for the density as a function of the fringes can be derived.[3]

In the three dimensional case, however, each fringe does not represent a change of air density only, but rather a change in the integral shown in equation (8), i.e., a change in the product of the variations of the index of refraction (and therefore air density) with the corresponding increment of light path and summed over the total light path. Equally spaced views around the field of interest are required by the HOLOFT program so that it can determine the density distribution. In the axisymmetrical or zero angle of attack case, however, only one view is required since all views should be the same and the program duplicates the one view for all the views it requires. This axisymmetrical case is the one that we have been testing.

The photograph of the cylinder with hemispherical cap at a Mach number of 0.8 and zero angle of attack (Figure 5) was digitized and the fringe distribution was entered into the program. The initial data reduction was

done only in the z = 0 plane (i.e., the cross section located at the tip of the model), because the stagnation air density at the tip is known. The program first calculates the distribution of the air density around the model and compares the calculated value at the tip of the model with the known value at the tip. It predicts the necessary shift in the fringe function required to enable it to calculate the known value at the tip. Next it recalculates the density distribution using the shifted fringe function. This process is repeated until the calculated and known densities at the tip converge. Convergence to within 1% is usually reached in only two or three iterations.

A theoretical calculation by Pulliam[10] has provided an air density distribution around this model for comparison with the output of the HOLOFT program to evaluate the accuracy of the holographic technique in the region near the model instead of just at the tip. It was found that "noise" in the fringe distribution had a significant effect on the results. Since the HOLOFT program uses the fringe data from only one side of the photograph in the axisymmetrical case, the data from both sides were averaged and smoothed graphically before being used in the program. It was found that small changes in the fringe distribution, especially at large radius, resulted in noticeable shifts in the calculated density distribution. This is because the integration paths are large at the large values of the radius. The process of finding the correct fringe number required many adjustments to the fringe distribution throughout the field of view in the z = 0 plane. The air density at the tip was calculated by the HOLOFT program as discussed above. The HOLOFT program also calculated the density distribution across the z = 0 plane and made a graph of this which was then compared with a graph of the corresponding calculation by Pulliam. Adjustments to

the fringe distribution were made and HOLOFT repeated the process. Then another comparison with Pulliam's calculation was made and another adjustment made to the fringe distribution. This process was repeated many times until there was a good match between the two plots.

The result of this experiment is shown[11] in the graph in Figure 11. The discrepancy at the origin is due to an artifact in the Pulliam code, not HOLOFT. This is a good match between Pulliam and HOLOFT, but it was necessary to raise the fringe number distribution N(x,y,o) by approximately 1 in this case. Because of "noise" in the fringe distribution the "zero" fringe at large distances away from the model cannot be numbered to within one fringe. Thus this method requires a reference density point such as the known stagnation density at the nose of the cylinder with hemispherical cap to define the "zero" fringe. Testing has begun at cross sections for other values of z for the axisymmetrical case.

These preliminary results reveal several difficulties that need to be addressed. As discussed above, the making of the interferograms during the reconstruction process is still largely an art. For instance, the decision on when to stop adjusting the micrometer screws on the dual plate holder is arbitrary, especially when "noise" in the fringe distribution is present. Figure 12 shows an interferogram containing a considerable amount of "noise" and "strangeness" in the fringe distribution. The fringes are not smooth curves, but contain many wiggles which indicate the presence of "noise". This is an axisymmetrical case, yet the fringes are not symmetrical about the axis of the model as they should be. In addition there are strange extra fringes that should not be there. Note the two closed loop fringes far in front of the model, another about one model diameter above the nose of the model and a fourth one about two model diameters below the

the model. Also note the vertical fringes near the rear of the model and the horizontal fringes below the model. It was not possible to eliminate these strange fringes during the reconstruction process without introducing other fringes that were even worse. The wiggles can be smoothed out by hand during the analysis, but what about the strange fringes? Should the loops be ignored? Are the loops the result of regions of higher or lower air density? It is not possible to determine which they are with an infinite fringe interferogram. The finite fringe interferogram can answer this question, however, by the direction that the fringes bend from straight lines.[2] The infinite fringes are easiest to count and the finite fringes provide information concerning the noise and turbulence, so both types of interferograms for each set of hologram plates are desirable. These closed loops even appeared in reconstructions of single plates that were "double pulsed", i.e., one plate exposed twice with the exposures only about 50 nanoseconds apart. This indicates that there must be a great deal of turbulence in the air flow before it reaches the model, especially for the Mach number 0.8.

The strange vertical and horizontal fringes near the edge mentioned above appeared in many of the interferograms. We have not yet located the cause of these, although it is possible that there was a slight change in the position of at least one of the optical elements between the times that the reference plates and the object plates were exposed at the wind tunnel since there is a lot of vibration when the wind tunnel is operating. Or perhaps some of the plate holders warped the plates slightly during the time they were exposed. It should be noted that the plate holders have a spring which pushes against the back side of the plate near its center to hold it firmly in place but the dual plate holder clamps the plates on only two of the edges so that a warping can take place during either the exposure or

or the reconstruction or both. This could introduce these unwanted spurious fringes when reconstructing two plates together since each would warp a little differently. The presence of these fringes makes it very difficult to determine when the interferogram has true infinite fringes without one or two finite fringes or even a fraction of a finite fringe superimposed on the fringe structure. Extra finite fringes superimposed on the infinite fringe structure could introduce an error in the calculated density.

A number of darkened regions are scattered randomly over the interferograms. They are located at the same places in all of the interferograms. They appear in the reconstruction of individual holograms so they are not caused by interference effects between the two plates. Several holograms were made during a test of the optical system when the windows were removed from the wind tunnel test section. There were no dark regions in the reconstructions of these. The windows were installed and holograms were made before the wind tunnel was put into operation. This time the dark regions appeared in the reconstructions. Therefore these dark regions must be caused by multiple reflections between the eight surfaces of the four windows. There may be slight variations in the thickness of the glass or its index of refraction. This effect does not change the fringe data but it does make it difficult to see in those regions. It can be reduced to some extent by proper "dodging" during the exposure of the interferogram.

Another question to consider is which fringe should be number zero? Ideally there would be no fringes far in front of the model, but the presence of noise, turbulence and the strange edge fringes makes it very difficult to determine where to start counting. For example, according to the results shown in Figure 11, the fringe we chose to label number "zero" should have been labelled number "one". Associated with this question is the related question of when to stop the adjustments of the micrometer screws during the

reconstructions. We always kept a bright region on the nose of the model, but perhaps it should have been a dark region instead or somewhere in between. The fringe numbering would then be off by a fraction of a fringe.

In the supersonic case shown in Figure 6 the air density in front of the shock wave should be constant so there should be no fringes in this region in the infinite fringe interferogram, and the fringes should be straight lines there in the finite fringe interferogram. Examination of these interferograms reveals, however, that there are fringes in front of the shock wave so the air density apparently is not uniform like it should be. Also a slight shock wave can be seen at the edge of the picture in front of the model. These effects indicate that there must be something in the wind tunnel upstream from the test section that is disturbing the air flow. In addition it was discovered that stray air currents passed through the object beam path in the region between the schlieren mirrors and the wind tunnel by the fans in the heating system of the building. Although these currents are slow, the beam path is long so turbulence and noise effects can be expected in the interferograms.

In addition, it had been anticipated that the shock wave touching the tip of the model in the supersonic case would cause so much disturbance that the fringes would be discontinuous where they cross the shock. This would make it very difficult or even impossible to number the fringes. Close examination of these interferograms reveals, however, that each fringe is continuous across the shock although it may be bent sharply. Thus the fringes can be numbered when appropriate care is exercised in the vicinity of the shock on the photograph. The effect of the shock is smaller than expected since the beam path through the region of the shock is actually quite short. The integral of equation (8) shows that the fringe number would thus remain fairly small so that the fringes should be continuous. This assumes that

the sudden change in the index of refraction at the shock does not cause any deviation of the light rays, but this is not true since shadowgraphs show a dark line at the shock indicating that the shock deviates the light rays at least a small amount. We assumed this deviation is so small that it would have no effect on the interferogram and so we ignored it.

Finally, a difficulty in the HOLOFT program became apparent early during the calculations. It proved to be very difficult to obtain the correct value of the air density at the tip of the model of the cylinder with hemispherical nose by adjusting the fringe distribution since a slight adjustment would cause a large change in the calculated density. The cause of the problem was that the important data points were concentrated in only a few of the available 101 locations in the computer and all the rest of the locations contained zero values. This happened because the significant fringe distribution is concentrated close to the model and very little relevant fringe information is located near the edges of the window. The problem was alleviated by inserting into the computer program values of the window radius, interferogram radius, laser beam radius and inversion circle radius that were much smaller than had been used previously. The original values were the actual physical dimensions while the new values were chosen to be just large enough to include the relevant data. This adjustment effectively spread the useful data over most of the 101 data locations thus giving the computer program more information with which to work so that the calculations gave much better values of the air density at the nose. The root cause of this problem, however, appears to be within the HOLOFT program itself. Apparently the evaluation of the inside integral over the radius is not as smooth as desired and the results are somewhat irregular so that the subsequent integration over the angles can be erratic. A recent test of the program in which the known air density was used to calculate the expected

fringe distribution which then was used to recalculate the air density resulted in a 15 percent error. Since this was a strictly theoretical exercise the error should have been very small so there must be a problem in the program. Yet in spite of this the good result shown in Figure 11 was obtained.

Conclusions and Recommendations

Holographic interferometry provides a non-invasive technique for estimating variations in the air density distribution around aerodynamic models in wind tunnels. The testing of this technique has been underway for some time and has been reported previously for a two-dimensional aerodynamic model.

This report summarizes results obtained from tests using three-dimensional aerodynamic models. Holograms have been made of aerodynamic models in a wind tunnel. Interferograms have been made from the holograms. The interference fringes in these holographic interferograms have been digitized and this information has been entered into the HOLOFT program. The HOLOFT program successfully calculated the known stagnation air density at the nose of a model and the known air density distribution across the cross-section passing through the stagnation point for the axisymmetrical case of this model at a mach number of 0.8. Thus the technique of holographic interferometry does work.

A number of difficulties arose during the course of this project ranging from shifting of the laser beam during the runs at the wind tunnel, to air turbulence, to difficulties in obtaining well shaped fringes while making the interferograms, to less accuracy than is desired in the HOLOFT program. A number of recommendations which should improve the results follow:

1. Refine the HOLOFT program so that the evaluation of the inside integral

over the radius is smoother. A first step would be to change the value of "np" from 101 to 151, or to 201 or even to 301. Although this change would increase the computation time, it would also provide more data points to the program and thus should smooth the results of the inside integral.

2. Estimate the amount of deviation suffered by the light rays as they pass through the shock wave around the pointed model. Determine if this effect is large enough to influence the fringe structure in the interferogram.

3. Make two new complete sets of interferograms, one with infinite fringes and the other with finite fringes, for one of the test cases using the hologram plates already available. Make use of the experience already gained to help in judging when the fringes have the best shape with the least amount of "strangeness". Information from the finite fringes will help with the evaluations of the infinite fringes.

4. Make another wind tunnel run using a larger diameter model of the cylinder with hemispherical cap. If the model were 4 inches in diameter, there should be at least twice as many fringes as with the present 2 inch model, yet the fringe pattern should still be small enough that it should not be influenced by the walls of the wind tunnel test section. The larger number of fringes should reduce the percent error caused by turbulance and strange fringes since these should not increase proportionately.

5. When making more wind tunnel runs, take great care to more effectively stop stray air currents in the optical path outside of the wind tunnel test section. This includes the optical path through the plenum chamber which may be several feet long and may contain strong air currents.

Also try to smooth the air flow through the test chamber or perhaps use a different wind tunnel.

6. Modify the glass plate holders by removing the spring that pushes against the back side of the center of the plate. It may be necessary to use other means to hold the glass plate firmly by its edges. In a separate test here at the University of the Pacific it was shown that the weight of only a 10 gram mass is sufficient to cause many fringes in a reflection interferogram using a 20 cm length of a white meter stick. Therefore the spring could cause considerable distortion of the glass plate and should be removed.

7. It should be possible to reduce the problem of the shifting laser beam which results in a misalignment with the pinhole when making the holograms. J. D. Trolinger[12] discusses the spatial filtering of high power pulsed lasers and indicates that usually compromises are necessary since the ideal pinhole would be destroyed in only a few pulses. Therefore he suggests using a larger pinhole which would still give a good degree of spatial filtering of the beam. Since the larger pinhole would result in a smaller Airy disk, the beam would not diverge enough to fill the entire window in the wind tunnel test section so another lens would be needed to expand the beam to the desired diameter.

The first two recommendations do not require any further experimental work, but can use the data already available. The third recommendation requires new reconstructions done in the laboratory from the existing holograms. The other recommendations involve making new holograms during wind tunnel runs.

Bibliography

1. Heflinger, L.O., Wuerker, R.F. and Brooks, R.E., "Holographic Interferometry", J. Appl. Phys., Vol. 37, pp. 642-649. 1966.
2. Vest, Charles M., Holographic Interferometry, Chapters 5 and 6, John Wiley and Sons. 1979.
3. Lee, George, "Application of Holography to Flow Visualization", NASA TM 84325, January 1984.
4. Craig, James E., Lee, George and Bachelo, William D., "Nd:YAG Holographic Interferometer for Aerodynamic Research", presented at the SPIE Conference on Industrial and Commercial Applications of Holography, San Diego, California, August 24-25, 1982, and published in SPIE Proceedings, Vol. 353.
5. Becker, Friedhelm and Yu, Yung, "Application of Digital Interferogram Techniques to the Measurements of Three-Dimensional Flow Fields", AIAA Aerospace Science Meeting, January 14-17, 1985, Reno, NV., Paper No. 0037.
6. Jenkins, Francis A. and White, Harvey E., Fundamentals of Optics, Fourth Edition, McGraw Hill, 1976.
7. Hecht, Eugene and Zajac, Alfred, Optics, Addison-Wesley, 1974.
8. Meyer-Arendt, Jurgen R., Introduction to Classical and Modern Optics, Second Edition, Prentice-Hall, 1984.
9. Van Houten, Paul Edgar, The Application of Holographic Interferometry to the Determination of Discontinuous Three-Dimensional Density Fields, Thesis for the degree of Aeronautical Engineer, Naval Postgraduate School, 1972.
10. Pulliam, Thomas H., "Implicit Finite Difference Simulations of Three-Dimensional Compressible Flows", AIAA J., Vol. 18, No. 2, pp. 159-167, 1980.

11. Perry, Richard L. and Lee, George, "Holographic Interferometry Applied to Symmetric Aerodynamic Models in a Wind Tunnel", presented at the SPIE Conference on Applications of Holography, Los Angeles, California, January 21-23, 1985, and published in SPIE Proceedings, Vol. 523, pp. 85-92.

12. Trolinger, J.D., "Laser Instrumentation for Flow Field Diagnostics", AGARD-AG-186, pp. 22-24, 1974.

Publications and Papers Read

1. Richard L. Perry and George Lee, "Holographic Interferometry Applied to Symmetric Aerodynamic Models in a Wind Tunnel", Proceedings of SPIE-The International Society for Optical Engineering, Vol. 523, pp. 85-92, 1985. (This was presented at SPIE's 1985 Los Angeles Technical Symposium on Optical & Electro-Optical Engineering, January 21, 1985.)

2. Richard L. Perry, "Holographic Interferometry: An Example in Aerodynamics", AAPT Announcer 12, No. 1, p. 69, March 1982. (AAPT Meeting at the University of the Pacific, Stockton, California, November 7, 1981.)

NOTE:

The earlier work was performed during the years of 1978-1983 under various IPA and University Consortium agreements numbered:

NCA2-0Y588-851

NCA2-0Y588-951

NCA2-04588-351

NCA2-0R588-001

NCA2-0R588-201

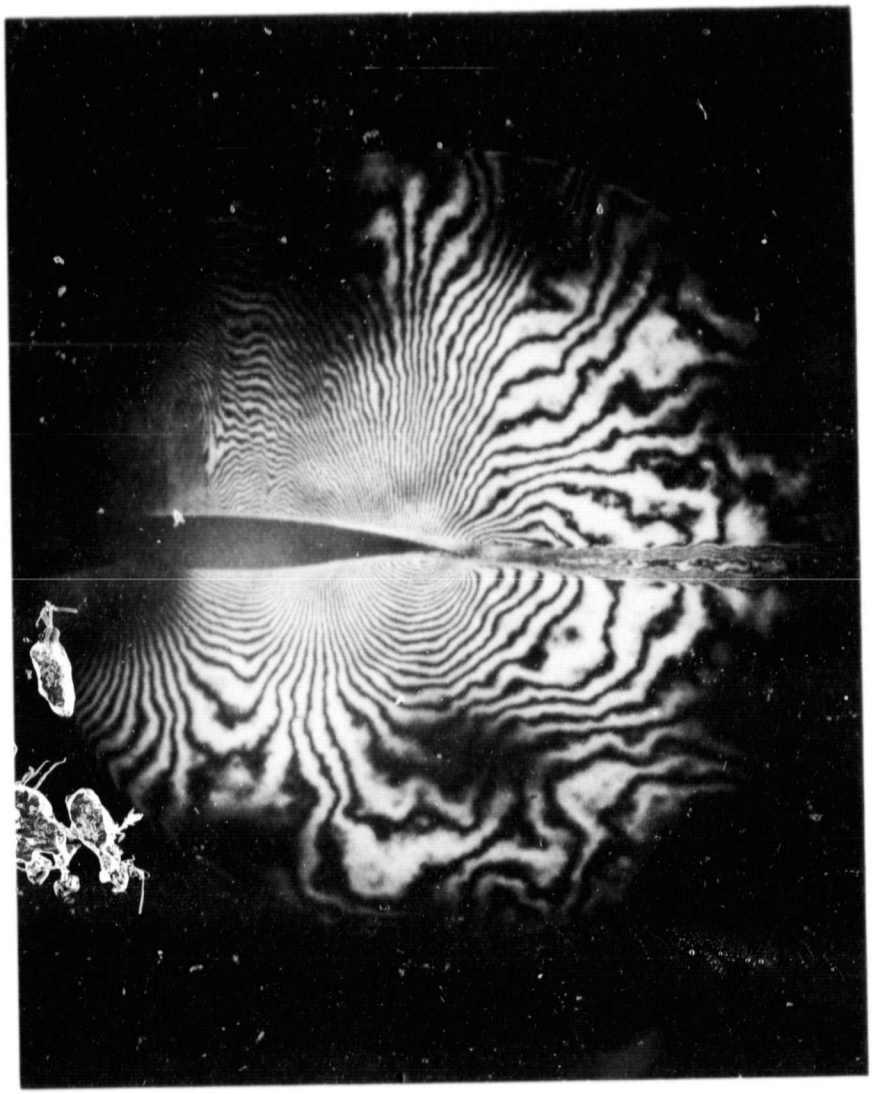

FIGURE 1.

INTERFEROGRAM OF A TWO-DIMENSIONAL WING.

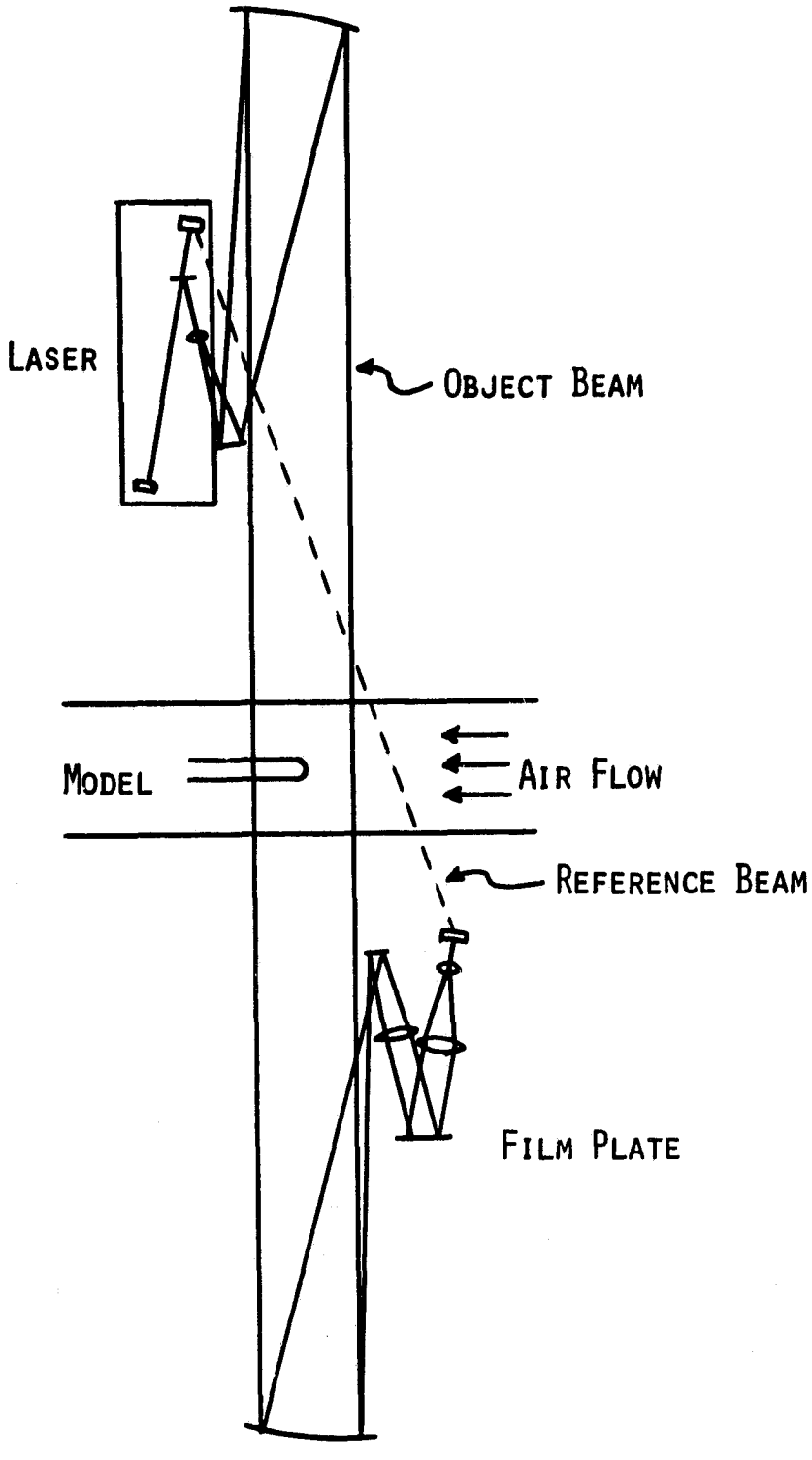

FIGURE 2.

SKETCH OF HOLOCAMERA.

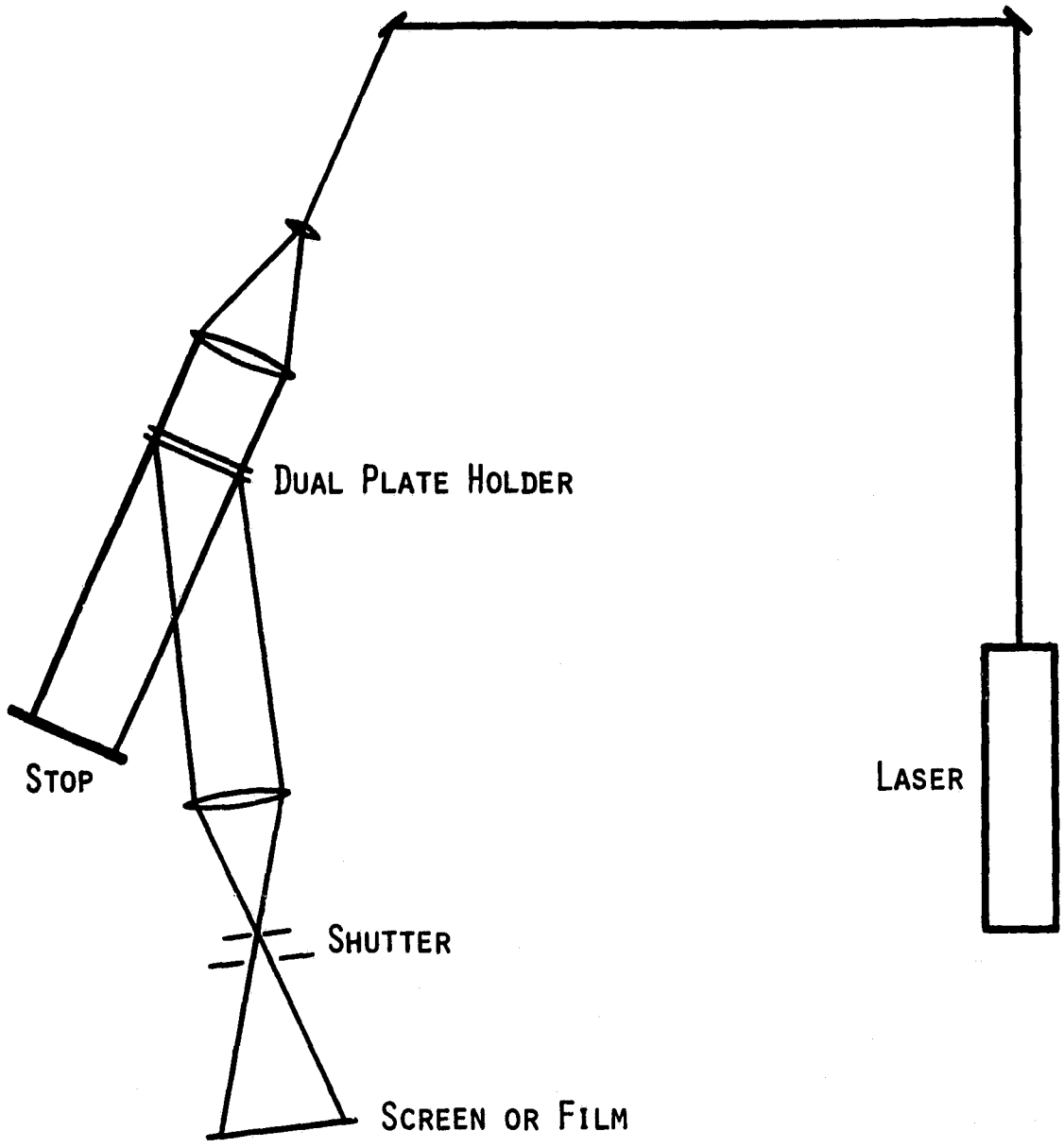

FIGURE 3.

SKETCH OF RECONSTRUCTION APPARATUS.

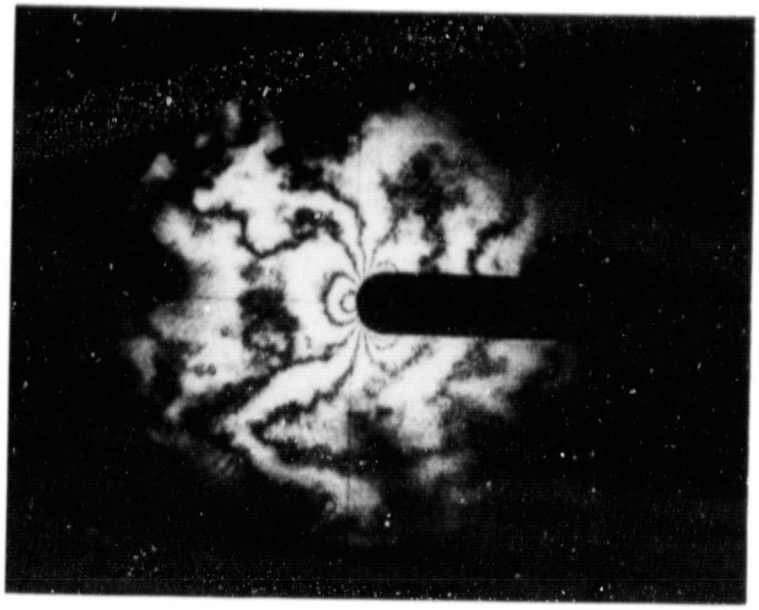

FIGURE 4.
INTERFEROGRAM OF CYLINDER WITH
HEMISPHERICAL CAP AT A MACH NUMBER OF 0.6.

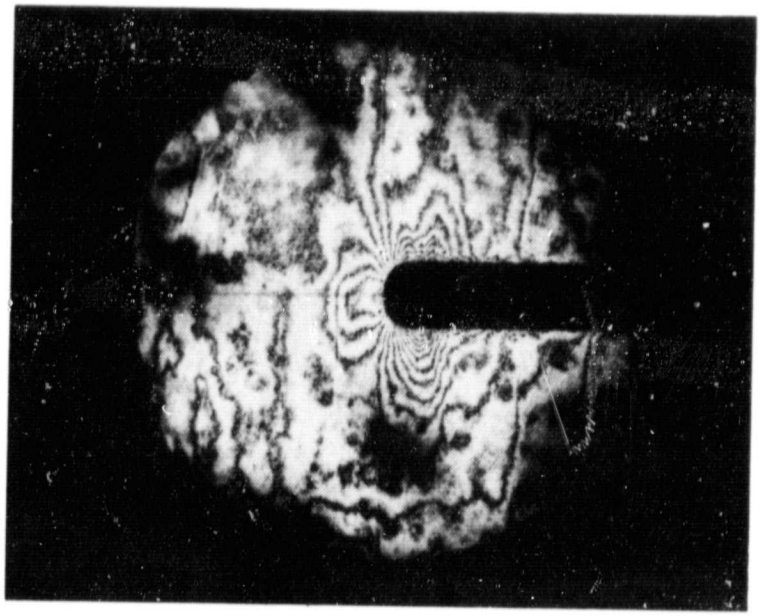

FIGURE 5.
INTERFEROGRAM OF CYLINDER WITH
HEMISPHERICAL CAP AT A MACH NUMBER OF 0.8.

(A) Infinite Fringe Mode

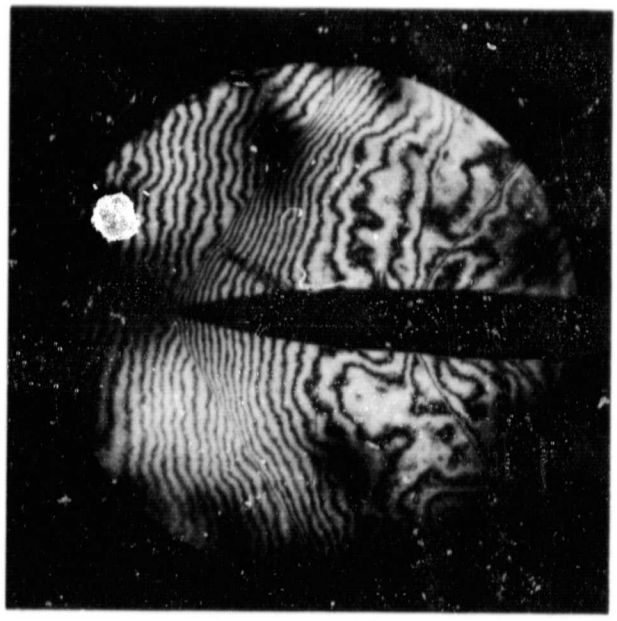

(B) Finite Fringe Mode

Figure 6.

Interferograms of pointed bump model at a Mach number of 1.25.

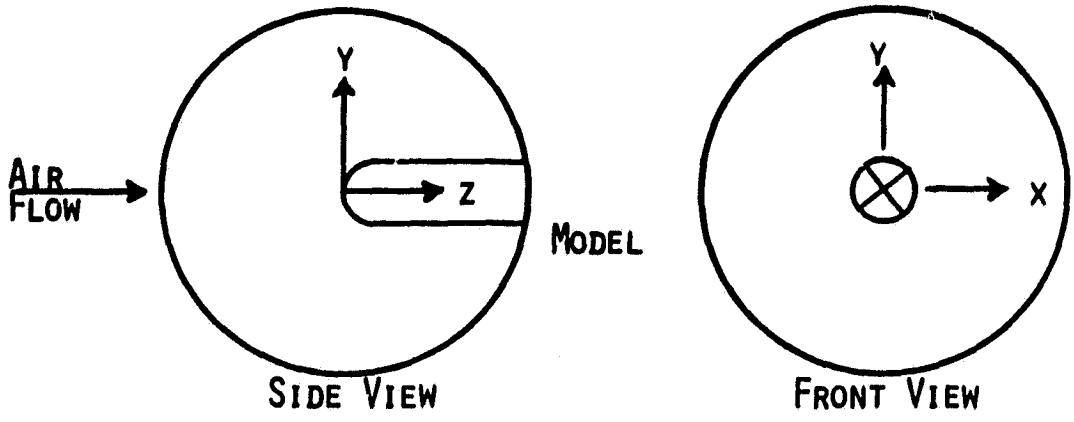

FIGURE 7.

DIAGRAM OF THE COORDINATE SYSTEM ATTACHED TO THE MODEL.

+90°, 0°, -90°

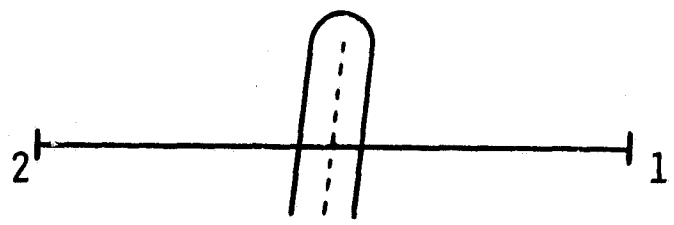

FIGURE 8.

DIAGRAM OF THE TRANSPARENT OVERLAY ON
THE INTERFEROGRAM AT AN ORIENTATION ANGLE OF -90°.

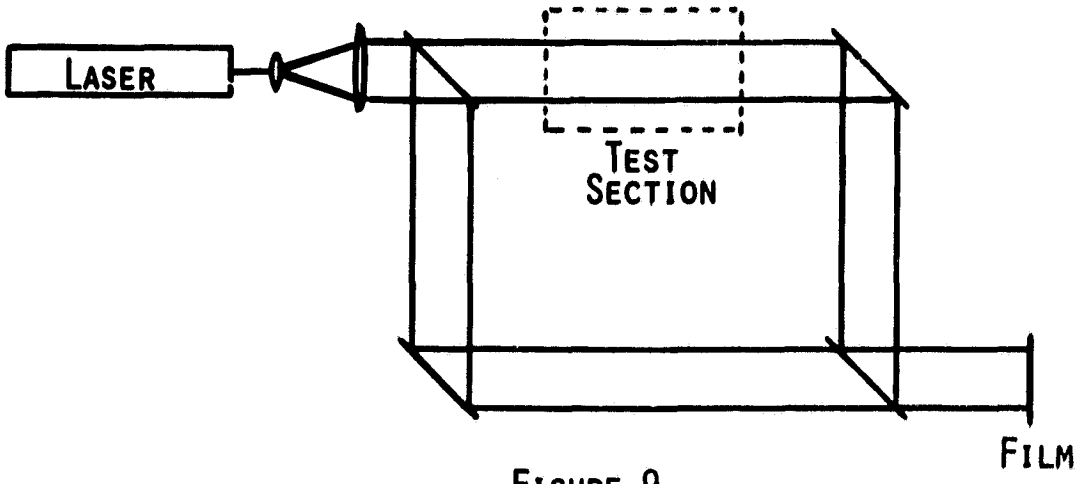

FIGURE 9.

DIAGRAM OF A MACH-ZEHNDER INTERFEROMETER.

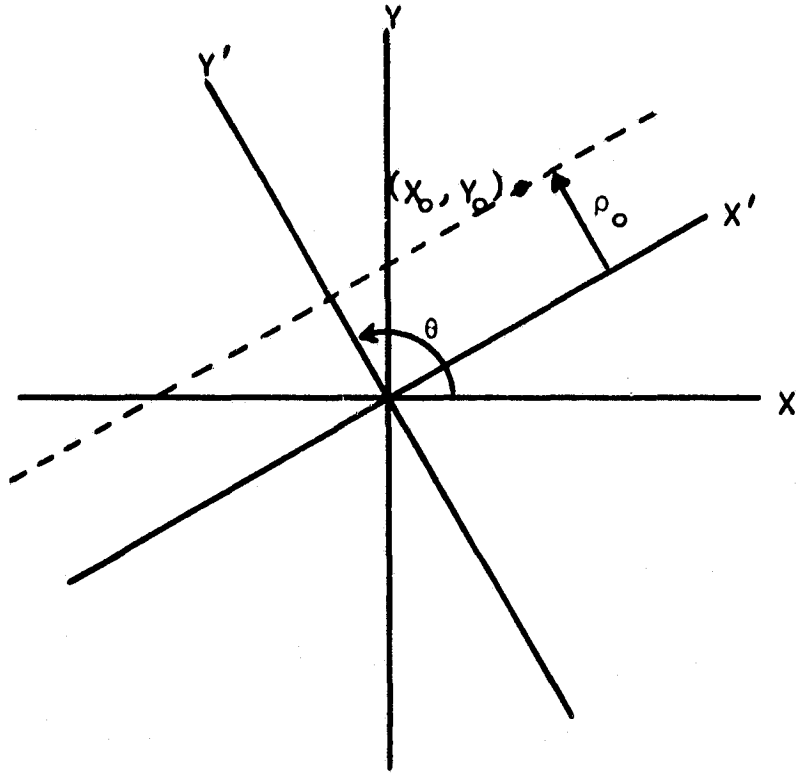

FIGURE 10.

DIAGRAM OF THE INVERSION COORDINATES.

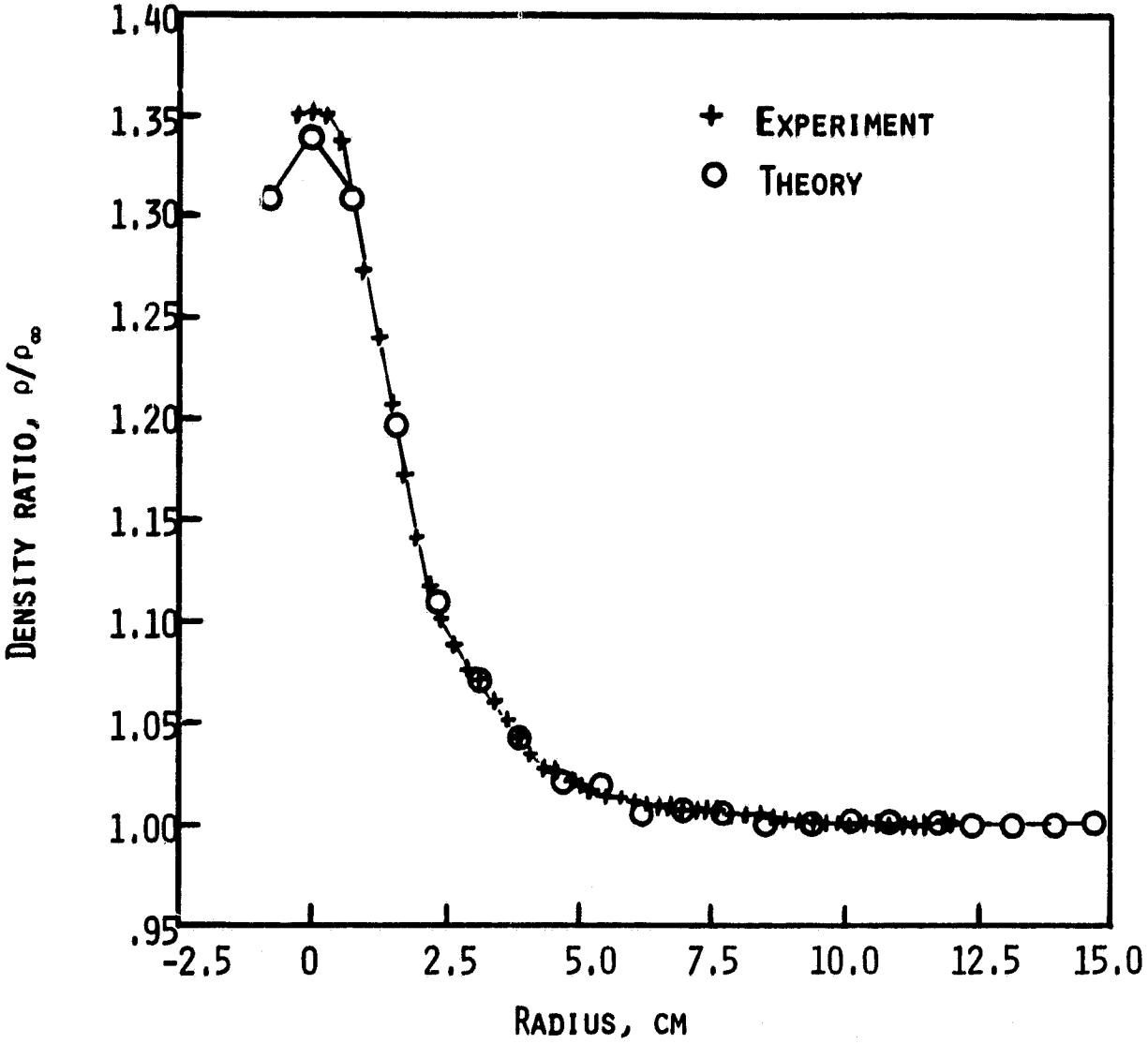

FIGURE 11.

PLOT OF HOLOFT CALCULATIONS COMPARED WITH THOSE FROM PULLIAM.

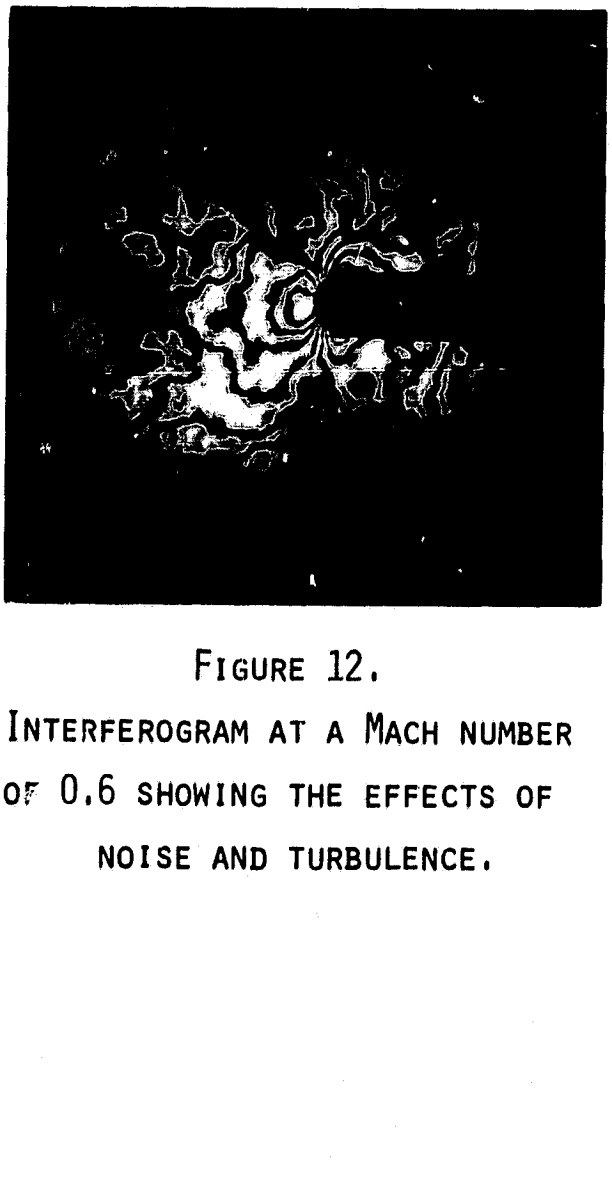

FIGURE 12.
INTERFEROGRAM AT A MACH NUMBER OF 0.6 SHOWING THE EFFECTS OF NOISE AND TURBULENCE.